

Polymer Translocation out of Planar Confinements

Debabrata Panja*, Gerard T. Barkema^{†,‡} and Robin C. Ball**

*Institute for Theoretical Physics, Universiteit van Amsterdam, Valckenierstraat 65, 1018 XE Amsterdam, The Netherlands

† Institute for Theoretical Physics, Universiteit Utrecht, Leuvenlaan 4, 3584 CE Utrecht, The Netherlands

‡Instituut-Lorentz, Universiteit Leiden, Niels Bohrweg 2, 2333 CA Leiden, The Netherlands

**Department of Physics, University of Warwick, Coventry CV4 7AL, UK

Abstract. Polymer translocation in three dimensions out of planar confinements is studied in this paper. Three membranes are located at $z = -h$, $z = 0$ and $z = h_1$. These membranes are impenetrable, except for the middle one at $z = 0$, which has a narrow pore. A polymer with length N is initially sandwiched between the membranes placed at $z = -h$ and $z = 0$ and translocates through this pore. We consider strong confinement (small h), where the polymer is essentially reduced to a two-dimensional polymer, with a radius of gyration scaling as $R_g^{(2D)} \sim N^{\nu_{2D}}$; here, $\nu_{2D} = 0.75$ is the Flory exponent in two dimensions. The polymer performs Rouse dynamics. Based on theoretical analysis and high-precision simulation data, we show that in the unbiased case $h = h_1$, the dwell-time τ_d scales as $N^{2+\nu_{2D}}$, in perfect agreement with our previously published theoretical framework. For $h_1 = \infty$, the situation is equivalent to field-driven translocation in two dimensions. We show that in this case τ_d scales as $N^{2\nu_{2D}}$, in agreement with several existing numerical results in the literature. This result violates the earlier reported lower bound $N^{1+\nu}$ for τ_d for field-driven translocation. We argue, based on energy conservation, that the actual lower bound for τ_d is $N^{2\nu}$ and not $N^{1+\nu}$. Polymer translocation in such theoretically motivated geometries thus resolves some of the most fundamental issues that are the subjects of much heated debate in recent times.

PACS numbers: 36.20.-r, 82.35.Lr, 87.15.Aa

1. Introduction

Polymer translocation through narrow pores in membranes is an active field of research in recent times: as a cornerstone of many biological processes, and also due to its relevance for practical applications. Molecular transport through cell membranes is an essential mechanism in living organisms. Often, the molecules are too long, and the pores in the membranes too narrow, to allow the molecules to pass through as a single unit. In such circumstances, the molecules have to deform themselves in order to squeeze — i.e., translocate — themselves through the pores. DNA, RNA and proteins are such naturally occurring long molecules [1–5] in a variety of biological processes. Translocation is also used in gene therapy [6, 7], in delivery of drug molecules to their activation sites [8], and as a potentially cheaper alternative for single-molecule DNA or RNA sequencing [9, 10].

In theoretical studies of translocation, the membrane is usually a stationary object that does not show any movement or fluctuations, and this also holds for the pore in it, through which translocation occurs. The polymer is usually simplified to a sequentially connected string of N monomers. A central quantity in these theoretical studies is the so-called dwell time τ_d , which is the time the pore remains blocked during a translocation event (Fig. 1).

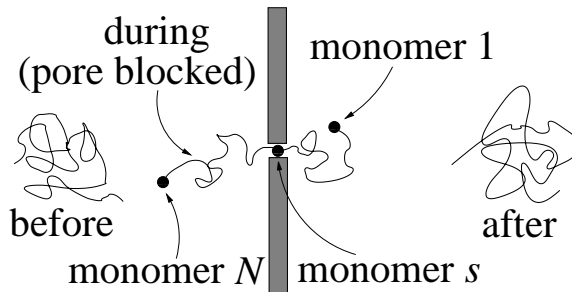


Figure 1. Pictorial representation of a translocation event, with the polymer shown before, during and after translocation. We number the monomers starting with the end monomer on the side it moves to. The number of the monomer located within the pore is s .

The early theories of translocation were constructed in the spirit of mean-field [14], and that too for phantom polymers, wherein translocation is quantified by a Fokker-Planck equation for first-passage over an entropic barrier in terms of a single “reaction coordinate” s . Here s is the number of the monomer threaded at the pore ($s = 1, \dots, N$), see Fig. 1. These mean-field type theories apply under the assumption that every translocation step is slower than the equilibration time-scale of the entire polymer. Some years ago, this assumption was questioned [15, 16], wherein the authors provided lower bounds for τ_d for three generic situations for phantom as well as self-avoiding polymers in the absence of hydrodynamical interactions:

- (a) Unbiased translocation (i.e., translocation in the absence of any driving field or

force on the polymer), for which $\tau_d \geq \tau_{\text{Rouse}}$, with $\tau_{\text{Rouse}} \sim N^{1+2\nu}$ being the Rouse time, the longest time-scale in the dynamics of the polymer;

- (b) Translocation driven by a field E , acting on the polymer only at the pore, for which it was shown that $\tau_d \geq N^{1+\nu}/E$;
- (c) Translocation effected by a pulling force F at the head of the polymer, for which it was shown that $\tau_d \geq N^2/F$.

Here, ν is the Flory exponent: in three dimensions $\nu \equiv \nu_{3\text{D}} \simeq 0.588$ and in two dimensions $\nu \equiv \nu_{2\text{D}} = 0.75$. Accompanying numerical studies led the authors to also suggest that the lower bounds indeed provide the correct scalings for τ_d ; and based on these results, they concluded that the dynamics of translocation, in (a-c), is anomalous [15, 16].

Subsequent numerical studies, however, did not immediately settle the scaling for τ_d with N . In Tables 1 and 2 we present a summary of results on the exponent for the scaling of τ_d with N (all results quoted are for self-avoiding polymers in the absence of hydrodynamical interactions in the scaling limit).

- (i) Unbiased translocation:

authors	two-dimensions	three-dimensions
Chuang <i>et al.</i> [15]	2.5	–
Luo <i>et al.</i> [17]	2.50 ± 0.01	–
Wei <i>et al.</i> [18]	2.51 ± 0.03	2.2
Klein Wolterink <i>et al.</i> [19]	–	2.40 ± 0.05
Milchev <i>et al.</i> [20]	–	2.23 ± 0.03
Dubbeldam <i>et al.</i> [21]	–	2.52 ± 0.04
Panja <i>et al.</i> [26]	–	$2 + \nu_{3\text{D}}$
This work	$2 + \nu_{2\text{D}}$	–

Table 1. Existing results on the exponent for the scaling of τ_d with N for unbiased translocation.

(ii) Field-driven translocation:

authors	two-dimensions	three-dimensions
Kantor <i>et al.</i> [16]	1.53 ± 0.01	–
Luo <i>et al.</i> [22]	1.72 ± 0.06	–
Cacciuto <i>et al.</i> [23] [†]	1.55 ± 0.04	–
Wei <i>et al.</i> [18]	–	1.27
Milchev <i>et al.</i> [20]	–	1.65 ± 0.08
Dubbeldam <i>et al.</i> [24]	–	1.5
This work	lower bound $2\nu_{2D}$; observed 1.5	–

Table 2. Existing numerical results on the exponent for the scaling of τ_d with N for field-driven translocation. The superscript [†] indicates that we discuss this paper in detail in the following paragraphs.

At a theoretical level, the lack of consensus on the scalings of τ_d can easily be attributed to the fact that none of the works in (i) and (ii) relates the numerically observed scaling of τ_d to the well-known dynamical features of polymers in a satisfactory manner. We do note here that Refs. [21, 24, 25] proposed to link the observed scalings of τ_d to anomalous dynamics of translocation via a fractional Fokker-Planck equation; but how this equation can be derived from the microscopic dynamics of a single polymer, as well as the assumptions underlying the form of this equation, remain entirely unclear.

In the recent past, this lack of consensus prompted us to investigate the microscopic origin of the anomalous dynamics for unbiased translocation. We set up a theoretical formalism, *based on the microscopic dynamics of the polymer*, and showed that the anomalous dynamics of translocation stem from the polymer’s memory effects [26, 27], in the following manner. Translocation proceeds via the exchange of monomers through the pore: imagine a situation when a monomer from the left of the membrane translocates to the right. This process increases the monomer density in the right neighbourhood of the pore, and simultaneously reduces the monomer density in the left neighbourhood of the pore. The local enhancement in the monomer density on the right of the pore *takes a finite time to dissipate away from the membrane along the backbone of the polymer* (similarly for replenishing monomer density on the left neighbourhood of the pore). The imbalance in the monomer densities between the two local neighbourhoods of the pore during this time implies that there is an enhanced chance of the translocated monomer to return to the left of the membrane, thereby giving rise to *memory effects*. The ensuing analysis enabled us to provide a proper microscopic theoretical basis for the anomalous dynamics, leading us to conclude that τ_d scales as $\sim N^{2+\nu_{3D}}$ for unbiased polymer translocation in three dimensions [26, 27].

In Refs. [26, 27] we also showed that the theory presented in Ref. [21] is not correct (which casts serious doubts about the correctness of a related theory presented

in the theoretically related paper Ref. [24]), but for unbiased translocation in three dimensions, the numerical result $\tau_d \sim N^{2.52 \pm 0.04}$ [21], obtained by the use of a polymer model very different from ours, is consistent with τ_d scaling as $\sim N^{2+\nu_{3D}}$. Two of us subsequently extended the theoretical formalism Refs. [26, 27] to analyze translocation by pulling the head of the polymer by a force F , leading to the theoretical derivation for $\tau_d \sim N^2/F$ [28].

The purpose of this paper is to push the theoretical formalism of Refs. [26–28] further to study translocation in three dimensions out of planar confinements for polymers performing Rouse dynamics. Clearly, confinement reduces the number of configurational states available to the polymer, reducing the polymer’s entropy and thereby increasing the polymer’s free energy [29, 30]. If the polymer is allowed to escape from the confinement through a pore, then it will translocate out of the confinement, and the free energy difference between the confined and the free state of the polymer will drive translocation. While confinement plays an important role for polymers in various biological processes [31], our interest in translocation out of planar confinement in this paper stems more from a theoretical point of view — we aim to demonstrate that our theoretical formalism [26, 27] works beautifully also in two dimensions. We divide the three-dimensional space into two parts: $z > 0$ and $z < 0$ by a membrane placed at $z = 0$. This membrane is impenetrable to the polymer except for a narrow pore. We then place two more parallel completely impenetrable membranes at $z = -h$ and $z = h_1$. The polymer is initially sandwiched between the membranes placed at $z = -h$ and $z = 0$. We only consider strong confinement of the polymer, i.e., $h \ll R_g^{(3D)}$, with the radius of gyration $R_g^{(3D)}$ for the polymer scaling in the present case as $\sim N^{\nu_{3D}}$. We study translocation out of planar confinement for two separate cases: (1) $h_1 = h$, and (2) $h_1 = \infty$. Our system for $h_1 = \infty$ is shown below in Fig. 2.

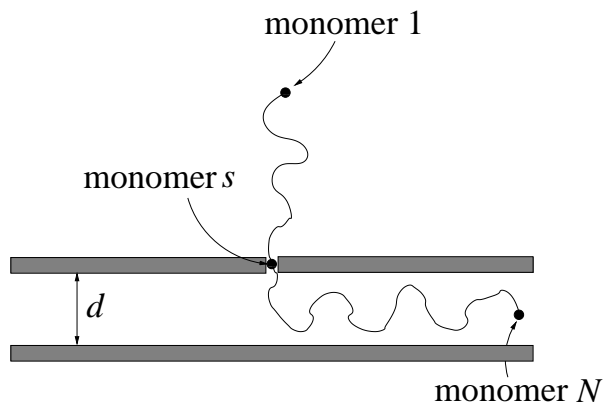


Figure 2. Our system, and a snapshot of a translocating polymer out of planar confinement, with $h_1 = \infty$. We use strong confinement, for which $h \ll R_g^{(3D)}$, where $R_g^{(3D)}$ is the radius of gyration for the polymer, scaling as $\sim N^{\nu_{3D}}$.

We substantiate our theoretical analysis with extensive Monte Carlo simulations, in which the polymer performs single-monomer moves. The definition of time is such

that single-monomer moves along the polymer's contour are attempted at a fixed rate of unity, while moves that change the polymer's contour are attempted ten times less often. Details of our self-avoiding polymer model in 3D can be found in Refs. [27, 32].

At strong confinements, i.e., with $h \ll N^{\nu_{3D}}$ the confined segment of the polymer essentially behaves as a two-dimensional polymer. We demonstrate this below for $h = 3$ (lattice units). We tether one end of the polymer of length $N/2$ at the pore on the membrane at $z = 0$, confine the polymer between the plates at $z = 0$ and $z = -h$, and measure the end-to-end distance R_e of the polymer in equilibrium, as well as the equilibrium correlation function of the end-to-end vector. That R_e scales as $(N/2)^{\nu_{2D}}$ and the equilibrium correlation function of the end-to-end vector behaves as $\exp[-t/\tau_{\text{Rouse}(2D)}]$ are demonstrated below in Table 3 and Fig. 3 respectively, with $\tau_{\text{Rouse}(2D)}$ being the Rouse time in two dimensions, scaling, for a polymer of length $N/2$, as $(N/2)^{1+2\nu_{2D}}$.

$N/2$	$\langle R_e \rangle$	$\langle R_e \rangle / (N/2)^{\nu_{2D}}$
100	10.248	0.324
150	13.759	0.321
200	17.135	0.322
250	20.242	0.322
300	23.171	0.321
350	26.213	0.324
400	28.872	0.323

Table 3. Average end-to-end distance for a polymer, confined between the membranes at $z = 0$ and $z = -h$, with one end tethered at the pore on the membrane at $z = 0$, for $h = 3$. The angular brackets denote an average over 10,000 runs for each N .

The confinement of a polymer of length N between the two planes at $z = 0$ and $z = -h$ is accompanied by an entropic (or free energy) cost of $\Delta F \sim Nh^{-1/\nu_{3D}}$ [30]. Thus, in the case that $h_1 > h$, the initial state of the polymer is entropically less favourable, and the polymer will escape through the pore to the wider space between the membranes at $z = 0$ and $z = h_1$. This process is analogous to field-driven translocation, with a field strength $\sim [h^{-1/\nu_{3D}} - h_1^{-1/\nu_{3D}}]$. Although this analogue has been correctly identified in Ref. [23], the interpretation of τ_d therein is not correct: Ref. [23] used ν_{3D} to describe the size of the confined polymer, while Table 3 and Fig. 3 clearly show that the scaling of the size of the confined polymer with length is characterised by the exponent ν_{2D} .

The proper interpretation of the numerical result of Ref. [23], therefore, clearly violates the lower bound $N^{1+\nu_{2D}}$, provided by Ref. [16] for τ_d . Table 2 shows more independent numerical evidence that the scaling of τ_d for field-driven translocation falls far short of $N^{1+\nu_{2D}}$. This raises serious doubts about the theoretical lower bound $N^{1+\nu}$ for τ_d for field-driven translocation argued in Ref. [16].

Our main results in this paper are two-fold. First, for $h_1 = h$, the entropic drive is absent; the translocation dynamics reduces to that of an unbiased translocation for a two-dimensional polymer. Based on theoretical analysis and high-precision simulation data, we show that the dwell time for a polymer of length N scales as $\tau_d \sim N^{2+\nu_{2D}}$ for $h_1 = h$, in perfect agreement with our previous results [26, 27]. In this paper, we actually go one step further than Refs. [26, 27] to show that the probability distribution of the dwell time, $P(\tau_d)$ for $h_1 = h$ has a scaling form $P(\tau_d) \sim \mathcal{P}(\tau_d/N^{2+\nu_{2D}})/N^{2+\nu_{2D}}$. Secondly, for field-driven translocation, we argue, based on conservation of energy, that the lower bound for τ_d for field-driven translocation is given by $N^{2\nu}$ in the absence of hydrodynamics. Using the analogue between translocation out of planar confinement for $h_1 = \infty$ and field-driven translocation in two dimensions, we demonstrate numerically that $\tau_d \sim N^{2\nu_{2D}}$, with our numerical results being consistent with those of Refs. [16] and [23]. Study of polymer translocation in these (theoretically motivated) geometries, therefore, is a fine test case for the fundamental physics governing translocation dynamics.

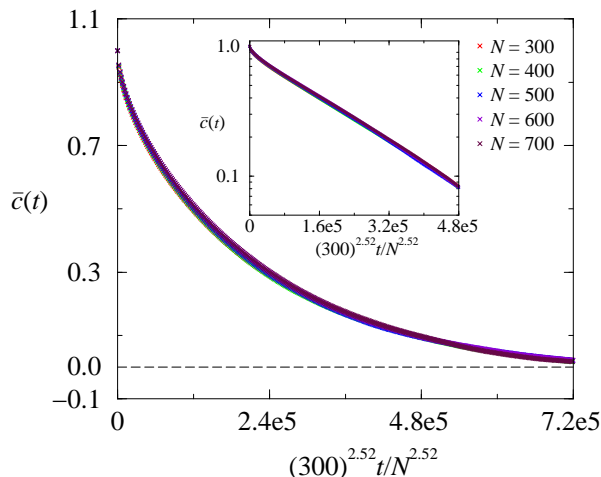


Figure 3. End-to-end equilibrium correlation function $\bar{c}(t)$ for a polymer with one end tethered at the pore on the membrane at $z = 0$, for $h = 3$. The data for each N are averaged over 256 realisations.

This paper is organised as follows. In Sec. 2 we discuss a method to measure $\Phi(t)$, the component of the polymer chain tension at the pore, perpendicular to the membrane. In Sec. 3 we analyze the memory effects in $\phi(t)$, the imbalance of the polymer chain tension across the pore. In Sec. 4 we discuss the consequence of these memory effects on unbiased translocation, i.e., for the case $h_1 = h$. In Sec. 5 we derive the lower bound $N^{2\nu}$ for τ_d for field-driven translocation, and discuss the consequence of this lower bound and the memory effects on translocation out of confinement for the case $h_1 = \infty$. We finally end this paper with a discussion in Sec. 6.

2. Chain tension at the pore perpendicular to the membrane

A translocating polymer can be thought of as two segments of polymers threaded at the pore, while the segments are able to exchange monomers between them through the pore. In Ref. [26] we developed a theoretical method to relate the dynamics of translocation to the imbalance of chain tension between these two segments across the pore. The key idea behind this method is that the exchange of monomers across the pore responds to the imbalance of chain tension $\phi(t)$; in its turn, $\phi(t)$ adjusts to $v(t)$, the transport velocity of monomers across the pore. Here, $v(t) = \dot{s}(t)$ is the rate of exchange of monomers from one side to the other, where $[s(t) - s(0)]$ is the total number of monomers translocated from one side of the pore to the other in time $[0, t]$. In fact, we noted that $[s(t) - s(0)]$ and $\phi(t)$ are conjugate variables in the thermodynamic sense, with $\phi(t)$ playing the role of the chemical potential difference across the pore.

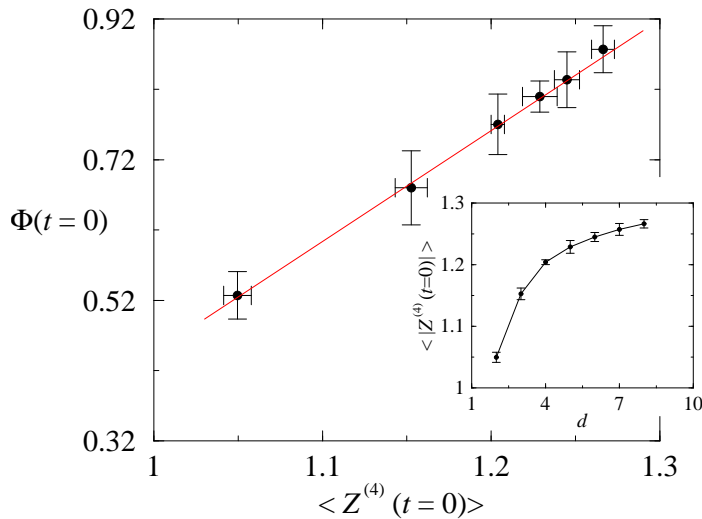


Figure 4. $\langle Z^{(4)}(t=0) \rangle$ vs. $\Phi(t=0)$ demonstrating the linear relationship between the two, for $N = 100$ and $h = 2, 3, 4, 5, 6$ and 8 respectively. The angular brackets for $\langle Z^{(4)}(t=0) \rangle$ indicate an average over 2,400 polymer realisations. The data for $\Phi(t=0)$ are obtained 2,400 polymer realisations as well. The solid line corresponds to the linear best-fit. Inset: $\langle Z^{(4)}(t=0) \rangle$ as a function of h .

By definition, $\phi(t) = \Phi_{z>0}(t) - \Phi_{z<0}(t)$ where $\Phi_{z>0}(t)$ and $\Phi_{z<0}(t)$ are respectively the chain tension (or the chemical potential) on the $z > 0$ and the $z < 0$ side of the pore. Consider a separate problem, where we tether one end of a polymer to a fixed membrane, yet the number of monomers are allowed to spontaneously enter or leave the tethered end, then we have

$$\frac{W_t(- \rightarrow +)}{W_t(+ \rightarrow -)} = \exp[\Phi(t)/k_B T], \quad (1)$$

where $W_t(- \rightarrow +)$ [resp. $W_t(+ \rightarrow -)$] is the rate that a monomer enters (resp. leaves) the polymer chain through the tethered end at time t . Note that tethering the polymer

while allowing monomers to enter or leave the polymer at the tethered end is precisely the case that translocation represents.

For a translocating polymer out of confinement between the membranes at $z = 0$ and $z = -h$, note that at $t = 0$, it is easy to use Eq. (1) to measure the chain tension for both segments at the pore [$\Phi(t = 0)$ in our notation], since under these conditions, we also have the relation that

$$P_- W_{t=0}(- \rightarrow +) = P_+ W_{t=0}(+ \rightarrow -), \quad (2)$$

where P_- (resp. P_+) is the probability that the $z < 0$ (or the $z > 0$) polymer segment has one monomer less (resp. one extra monomer). Equations (1) and (2) together yield us

$$\Phi(t = 0) = k_B T \ln \frac{P_+}{P_-}. \quad (3)$$

The chain tension as obtained from Eq. (3) is linearly related to the distance of the centre-of-mass of the first few monomers along the polymer's backbone, at the immediate vicinity of the pore, at least in our simulations. This is shown in Fig. 4, where for a tethered polymer of length $N = 100$, the average distance $\langle Z^{(4)}(t = 0) \rangle$ of the centre-of-mass of the first 4 monomers along the polymer's backbone from the membrane, counting from the tethered end of a polymer, is plotted versus the chain tension Φ , for a variety of h values. Within the error bars, all the points in Fig. 4 fall on a straight line, implying that Φ is very well-proxied by $\langle Z^{(4)} \rangle$. Since measurements of the chain tension via Eq. (3) are much more noisy than measurements of $\langle Z^{(4)} \rangle$, we will use the latter quantity as a measure for the chain tension.

3. Memory effects in the z -component of the chain tension at the pore

In the case of unbiased polymer translocation, we have witnessed in Refs. [26,27] that the memory effects of the polymer give rise to anomalous dynamics of translocation. We argued [26,27] that the velocity of translocation $v(t) = \dot{s}(t)$, representing monomer current, responds to $\phi(t)$, the imbalance in the monomeric chemical potential across the pore acting as ‘‘voltage’’. Simultaneously, $\phi(t)$ also adjusts in response to $v(t)$. In the presence of memory effects, they are related to each other by $\phi(t) = \phi_{t=0} + \int_0^t dt' \mu(t - t')v(t')$ via the memory kernel $\mu(t)$, which can be thought of as the (time-dependent) ‘‘impedance’’ of the system.

In this section, following Refs. [26,27] we determine the memory kernel $\mu(t)$ to describe the dynamics of translocation out of (strong) planar confinements. Note that for the case $h_1 = h$, there is an obvious symmetry between the polymer segments confined within the parallel plates below and above the $z = 0$ plane, implying that the corresponding memory kernels denoted by $\mu_{z>0}^{(h)}(t)$ and $\mu_{z<0}^{(h)}(t)$ are the same. For the case $h_1 = \infty$, we already know the form of $\mu_{z>0}^{(\infty)}(t)$ from Ref. [26,27]. In fact, in Ref. [26] we determined $\mu_{z>0}^{(\infty)}(t)$ by injecting p monomers into the tethered end of an equilibrated, tethered polymer of length $N/2 - p$ (bringing the total length to $N/2$), and proxying

$\phi(t)$ by the average distance of the centre-of-mass of the first 4 monomers $\langle Z^{(4)}(t) \rangle$ from the membrane. We found

$$\mu_{z>0}^{(\infty)}(t) \sim t^{-\frac{1+\nu_{3D}}{1+2\nu_{3D}}} \exp[-t/\tau_{\text{Rouse}(3D)}], \quad (4)$$

with $\tau_{\text{Rouse}(3D)}$ is the Rouse time for a polymer of length $N/2$, i.e., $\tau_{\text{Rouse}(3D)} \sim (N/2)^{1+2\nu_{3D}}$.

Following Refs. [26, 27], here we compute $\mu_{z<0}^{(h)}(t)$, the memory effect of a polymer of length $N/2$ with one end tethered to the pore in the membrane placed at $z = 0$. Indeed, the expression for $\mu_{z<0}^{(h)}(t)$, as we derive below, is given by

$$\mu_{z<0}^{(\infty)}(t) \sim t^{-\frac{1+\nu_{2D}}{1+2\nu_{2D}}} \exp[-t/\tau_{\text{Rouse}(2D)}]. \quad (5)$$

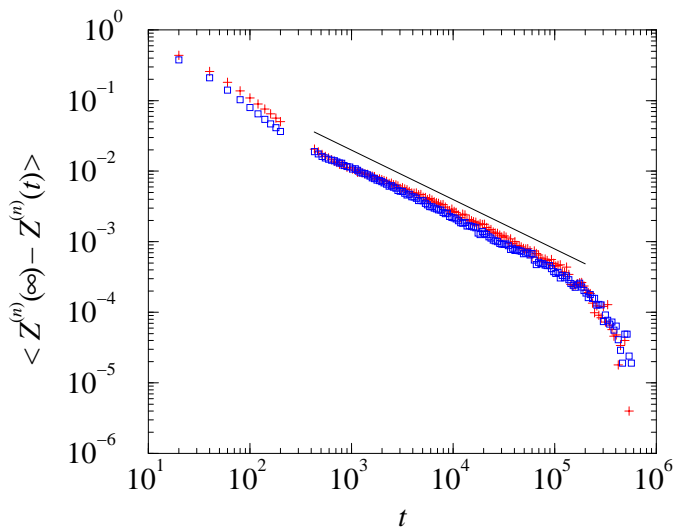


Figure 5. $\langle Z^{(4)}(\infty) - Z^{(4)}(t) \rangle$ for $N/2 = 250$, for $h = 3$ (pluses) and $h = 2$ (squares). The solid line corresponds to the power law $t^{-(1+\nu_{2D})/(1+2\nu_{2D})}$. Note that the data for $h = 2$ obeys a cleaner power law $t^{-(1+\nu_{2D})/(1+2\nu_{2D})}$ than the data for $h = 3$: this we can expect, as the polymer resembles a two-dimensional polymer more for $h = 2$ than for $h = 3$. The angular brackets correspond to 3, 200, 000 polymer realisations.

While the Rouse relaxation $\exp[-t/\tau_{\text{Rouse}(2D)}]$ can be easily justified based on Fig. 3, the value of α for $\mu_{z<0}^{(\infty)}(t) \sim t^{-\alpha} \exp[-t/\tau_{\text{Rouse}(2D)}]$ is obtained by following the procedure of Refs. [26, 27]. The value of α depends on the relaxation properties following the event of injecting, say, p extra monomers at the tether end, just like extra monomers add to (or get taken out of) the polymer segment confined within $z < 0$ during translocation. Given the $\exp[-t/\tau_{\text{Rouse}(2D)}]$ behaviour of Fig. 3, we anticipate that by time t after the extra monomers are injected at the tethered point, the extra monomers will come to a steady state across the inner part of the polymer up to $n_t \sim t^{1/(1+2\nu_{2D})}$ monomers from the tethered point, but not significantly further. This internally equilibrated section of $n_t + p$ monomers extends only $r(n_t) \sim n_t^{\nu_{2D}}$, less than its equilibrated value $(n_t + p)^{\nu_{2D}}$, because the larger scale conformation has yet to adjust: the corresponding compressive

force from these $n_t + p$ monomers is expected by standard polymer scaling [30] to follow $f/(k_B T) \sim \delta r(n_t)/r^2(n_t) \sim \nu_{2D} p / [n_t r(n_t)] \sim t^{-(1+\nu_{2D})/(1+2\nu_{2D})}$, for $p \ll n_t$. As was the case in Refs. [26–28], we expect that the chain tension at the pore behaves linearly with the force f , leading to $\alpha = (1 + \nu_{2D})/(1 + 2\nu_{2D}) = 0.7$.

We have confirmed this picture by measuring the impedance response through simulations. In Fig. 4, we have shown that the centre-of-mass of the first few monomers is an excellent proxy for chain tension at the pore and we assume here that this further serves as a proxy for $\delta\Phi$. Based on this idea, we track $\langle \delta\Phi^{(z<0)}(t) \rangle$ by measuring $\langle Z^{(4)}(t) \rangle$, in response to the injection of extra monomers near the pore at time $t = 0$. Specifically we consider the equilibrated segment of the polymer confined within $z < 0$, of length $N/2 - 5$ (with one end tethered at the pore), adding 5 extra monomers at the tethered end of the polymer segment at time $t = 0$, corresponding to $p = 5$, bringing its length up to $N/2$. Using the proxy $\langle Z^{(4)}(t) \rangle$, we then track $\langle \delta\Phi^{(z<0)}(t) \rangle$. At short times, these p monomers quickly expand in the z -direction (e.g., $t \lesssim 400$ in Fig. 5). Only after they “feel” the impenetrable membrane at $z = -h$, they turn around to expand along the xy -plane: indeed, the agreement between the latter and the theoretical prediction of $\alpha = (1 + \nu_{2D})/(1 + 2\nu_{2D})$ for $t \gtrsim 400$, for $N/2 = 250$, and for $h = 2$ and 3, can be seen in Fig. 5. Note that the sharp deviation of the data from the power law $t^{-(1+\nu)/(1+2\nu)}$ at long times is due to the asymptotic exponential decay as $\exp[-t/\tau_{\text{Rouse}(2D)}]$ of $\langle \delta\Phi^{(z<0)}(t) \rangle$ at long times. See also Fig. 2 of Ref. [26] in this context.

4. The case $h_1 = h$: consequence of the polymer’s memory effects on unbiased translocation

For the case $h_1 = h$ the condition $\mu_{z>0}^{(h)}(t) = \mu_{z<0}^{(h)}(t) \equiv \mu^{(h)}(t)$ for the polymer segments above and below the plane $z = 0$ allows us to write $\phi(t) = \phi_{t=0} + \int_0^t dt' \mu^{(h)}(t-t')v(t')$, as presented in the starting paragraph of Sec. 3. Supposing a zero-current equilibrium condition at time $t = 0$, this relation can be inverted to obtain $v(t) = \int_0^t dt' a(t-t')\phi(t')$, where $a(t)$ can be thought of as the “admittance”. In the Laplace transform language, $\tilde{\mu}^{(h)}(k) = \tilde{a}^{-1}(k)$, where k is the Laplace variable representing inverse time. Via the fluctuation-dissipation theorem, they are related to the respective autocorrelation functions as $\mu^{(h)}(t-t') = \langle \phi(t)\phi(t') \rangle_{v=0}$ and $a(t-t') = \langle v(t)v(t') \rangle_{\phi=0}$.

As explained in the introduction, translocation for $h_1 = h$ is unbiased, for which, having shown that $\mu^{(h)}(t) \sim t^{-\frac{1+\nu_{2D}}{1+2\nu_{2D}}} \exp[-t/\tau_{\text{Rouse}(2D)}]$, we expect [26, 27] that the translocation dynamics is anomalous for $t < \tau_{\text{Rouse}(2D)}$, in the sense that the mean-square displacement of the monomers through the pore, $\langle \Delta s^2(t) \rangle \sim t^\beta$ for some $\beta < 1$ and time $t < \tau_{\text{Rouse}(2D)}$, whilst beyond the Rouse time it becomes simply diffusive. Strictly speaking, $\tau_{\text{Rouse}(2D)}$ in this expression should be replaced by the characteristic equilibration time of a tethered polymer with length of $O(N)$; since both scale as $N^{1+2\nu_{2D}}$, we use $\tau_{\text{Rouse}(2D)}$ here, favouring notational simplicity. The value $\beta = \alpha = \frac{1+\nu_{2D}}{1+2\nu_{2D}}$ follows trivially by expressing $\langle \Delta s^2(t) \rangle$ in terms of (translocative) velocity correlations $\langle v(t)v(t') \rangle$, which (by the Fluctuation Dissipation

theorem) are given in terms of the time dependent admittance $a(t - t')$, and hence inversely in terms of the corresponding impedance. In other words, up to the Rouse time, the squared displacement as a function of time is subdiffusive, following $\langle \Delta s^2(t) \rangle \sim t^{\frac{1+\nu_{2D}}{1+2\nu_{2D}}}$. Consequently, at the Rouse time $\tau_{\text{Rouse}(2D)} \sim N^{1+2\nu_{2D}}$, the squared displacement scales as $\langle \Delta s^2[\tau_{\text{Rouse}(2D)}] \rangle \sim N^{1+\nu_{2D}}$. Beyond the Rouse time, there are no memory effects and the squared displacement increases linearly in time: $\langle \Delta s^2(t) \rangle \sim \{ \langle \Delta s^2[\tau_{\text{Rouse}(2D)}] \rangle / \tau_{\text{Rouse}(2D)} \} t \sim N^{-\nu_{2D}} t$. Based on the criterion for unthreading, i.e., unthreading occurs when $\sqrt{\langle \Delta s^2(\tau_d) \rangle} \sim N$, one then obtains $\tau_d \sim N^{2+\nu_{2D}}$ [26, 27].

N	τ_u	$\tau_u/N^{2+\nu_{2D}}$	$\tau_u/N^{1+2\nu_{2D}}$
30	2439	0.2114	0.4948
40	5176	0.2034	0.5115
50	9499	0.2021	0.5373
60	15684	0.2021	0.5624
70	24532	0.2069	0.5984
80	34556	0.2018	0.6037
90	47974	0.2027	0.6243
100	64755	0.2048	0.6476
200	415767	0.1954	0.7350
300	1268463	0.1955	0.8137
400	2765246	0.1932	0.8641
500	4961331	0.1877	0.8875
600	8228721	0.1885	0.9332
700	12648891	0.1897	0.9758
800	17975330	0.1867	0.9930

Table 4. Median values of τ_u based on 8,192 unthreading realisations for each N .

For computer simulations of unbiased translocation in two dimensions, Luo et al. [17] reported a scaling of $\tau_d \sim N^{1+2\nu_{2D}}$; note that this exponent and our theoretical expectation is 10% different. To distinguish these two different exponents, we performed high-precision simulations to obtain the unthreading time for a number of N -values: $N = 30, 40, 50, 60, 70, 80, 90, 100, 200, 300, 400, 500, 600, 700, 800$, for 8,192 realisations for each value of N , with a membrane spacing of $h = 3$ (Table 4). The unthreading time τ_u in Table 4) is defined as the time for the polymer to leave the pore with $s(t = 0) = N/2$ and the two polymer segments equilibrated at $t = 0$. Both τ_u and τ_d scale the same way, since $\tau_u < \tau_d < 2\tau_u$ [27]. The data of Table 4, along with the effective exponent for τ_u vs. N as a power law are further shown in Fig. 6. To be able to use the full potential of the statistics of 8,192 realisations for each N , we also plot the sorted $\tau_u/N^{2+\nu_{2D}}$ and $\tau_u/N^{1+2\nu_{2D}}$ vs. the normalised rank of the sorted values in Fig. 7. The data collapse is a further test that rules out the τ_d scaling as $N^{1+2\nu_{2D}}$, as reported in Ref. [15, 17, 18]: in fact the left panel of Fig. 7 suggests that $P(\tau_d)$, the probability distribution for the dwell

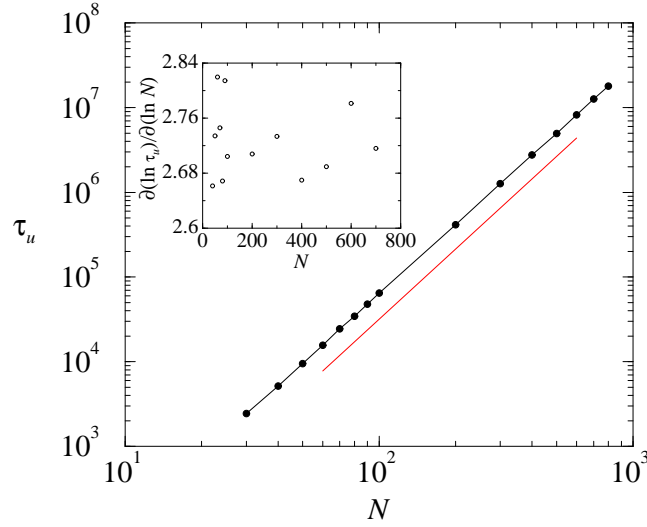


Figure 6. Scaling of τ_u with N : τ_u data of Table 4 are represented by the black line with points, solid line corresponds to the scaling $\tau_u \sim N^{2+\nu_{2D}}$. The effective exponents $\partial(\ln \tau_u)/\partial(\ln N)$ for $N = 40, 50, 60, 70, 80, 90, 100, 200, 300, 400, 500, 600, 700$ are shown in the inset, clearly ruling out $N^{1+2\nu_{2D}}$ scaling of τ_u in favour of $N^{2+\nu_{2D}}$.

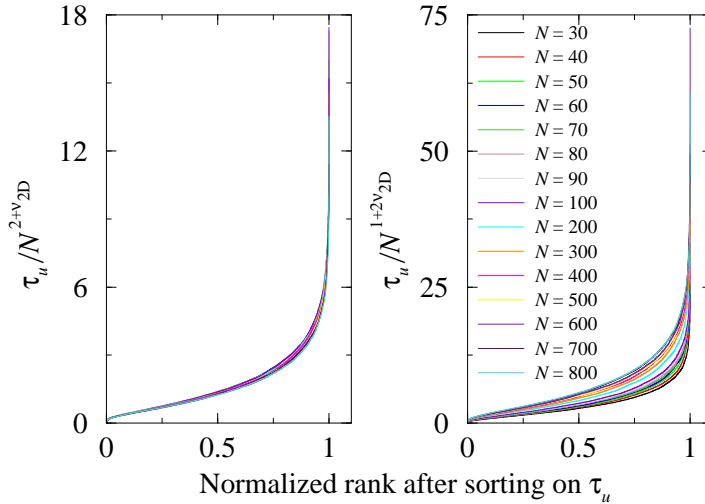


Figure 7. Sorted values $\tau_u/N^{2+\nu_{2D}}$ and $\tau_u/N^{1+2\nu_{2D}}$ vs. their normalised rank, for 8,192 realisations per value of N . Data shown (from bottom to top in the right panel): $N = 30, 40, 50, 60, 70, 80, 90, 100, 200, 300, 400, 500, 600, 700, 800$. The left panel shows a much better collapse than the right panel, ruling out the τ_d scaling as $N^{1+2\nu_{2D}}$, as observed by Luo et al. [17]. In fact, the data collapse in the left panel suggests that $P(\tau_d)$, the probability distribution for the dwell time τ_d has a scaling form $P(\tau_d) \sim \mathcal{P}(\tau_d/N^{2+\nu_{2D}})/N^{2+\nu_{2D}}$, with a scaling function $\mathcal{P}(x)$.

time τ_d has a scaling form $P(\tau_d) \sim \mathcal{P}(\tau_d/N^{2+\nu_{2D}})/N^{2+\nu_{2D}}$, with a scaling function $\mathcal{P}(x)$. These results together clearly demonstrate that the dwell time scales as $\tau_d \sim N^{2+\nu_{2D}}$.

5. τ_d for $h_1 = \infty$, or equivalently, τ_d for field-driven translocation in two dimensions

5.1. Lower bound for τ_d for field-driven translocation

We now turn to the case $h_1 = \infty$, which is equivalent to field-driven translocation in two dimensions as we discussed in the introduction. For our first stop, we notice in Table 2 that quite a few reported numerical results violate the lower bound $N^{1+\nu}$ for the scaling exponent of τ_d , suggested in Ref. [16], including that of the authors of Ref. [16] themselves. In light of this, below we first discuss the lower bound for field-driven translocation.

The crux of the derivation of the lower bound for τ_d in Ref. [16] is that, with or without an applied field, the mobility of a polymer translocating through a narrow pore in a membrane will not exceed that of a polymer in bulk (i.e., in the absence of the membrane). To obtain the mobility of a polymer in bulk, the authors assumed two more attributes of a polymer under a driving field:

- (i) To mimic the action of a field on a translocating polymer, the field on the polymer in bulk has to act on a monomer whose position along the backbone of the polymer changes continuously in time. As a result, there is no incentive for the polymer to change its shape from its bulk equilibrium shape, i.e., the polymer can still be described by a blob with radius of gyration $\sim N^\nu$ in the appropriate dimension.
- (ii) The polymer's velocity is $\sim mE$, where E is the field, and m is the mobility $\sim 1/N$.

Of these two assumptions, note that (ii) is obtained as the steady state solution of the equation of motion of a Rouse polymer, in bulk, with uniform velocity and vanishing internal forces (see e.g., Ref. [30], Eq. VI.10). We have already witnessed in many occasions [15, 16, 21, 24–28] that the dynamics of translocation through a narrow pore is anomalous (subdiffusive), and in Sec. 3 of this paper we have seen that there are strong memory effects in the polymer, to the point that the velocity of translocation is not constant in time. The anomalous dynamics and the memory effects are crucial ingredients that question the validity of the lower bound $N^{1+\nu}$ for τ_d for field-driven translocation.

A lower bound for τ_d for field-driven translocation does nevertheless exist, and it can be obtained from conservation of energy. Consider a translocating polymer under an applied field E which we can assume to be acting only at the pore: N monomers take time τ_d to translocate through the pore. The total work done by the field in time τ_d is then given by EN . In time τ_d , each monomer travels a distance of $\sim R_g$, leading to an *average* monomer velocity $v_m \sim R_g/\tau_d$. The rate of loss of energy due to viscosity η of the surrounding medium per monomer is given by ηv_m^2 . For a Rouse polymer, the frictional force on the entire polymer is a sum of frictional forces on individual monomers, leading to the total free energy loss due to the viscosity of the surrounding medium during the entire translocation event scaling as $\Delta F \sim N\tau_d\eta v_m^2 = N\eta R_g^2/\tau_d$.

This loss of energy must be less than or equal to the total work done by the field EN , which yields us the inequality $\tau_d \geq \eta R_g^2/E = \eta N^{2\nu}/E$ [33].

5.2. τ_d for the case $h_1 = \infty$

If we follow the procedure due to two of us in Ref. [28] to calculate τ_d for the case $h_1 = \infty$ via the memory kernels discussed in Sec. 3, then we would adopt the following route. For the translocated part of the polymer (in the space $z > 0$), the memory kernel takes the form of Eq. (4), while the translocating part of the polymer (in the space $z < 0$ and $z > -h$) the memory kernel takes the form of Eq. (5). Of these, the magnitude of the exponent in the power law of Eq. (5) is less than that of Eq. (4) [i.e., the memory effects of the translocating part of the polymer are longer-lived than that of the translocated part of the polymer], which implies that the relation between the chain tension imbalance across the pore and translocation velocity should be described by the equation

$$\phi(t) = \phi_{t=0} - \int_0^t dt' |\mu_{z<0}^{(\infty)}(t-t')| v(t'), \quad (6)$$

leading to

$$v(t) = \int_0^t dt' (t-t')^{-(1+3\nu_{2D})/(1+2\nu_{2D})} [\phi(0) - \phi(t')], \quad (7)$$

via Laplace transform [28]. Furthermore, if $[\phi(0) - \phi(t')]$ remains a constant (not shown here [34]), then Eq. (7) yields $v(t) \sim t^{-\nu_{2D}/(1+2\nu_{2D})}$, implying that the distance $[s(t) - s(0)]$ unthreaded in time t should behave as $s(t) = s(0) + \int_0^t dt' v(t') \sim t^{(1+\nu_{2D})/(1+2\nu_{2D})}$. With $[s(\tau_d) - s(0)] = N$, the relation $[s(t) - s(0)] \sim t^{(1+\nu_{2D})/(1+2\nu_{2D})}$ would finally yield $\tau_d \sim N^{(1+2\nu_{2D})/(1+\nu_{2D})}$.

The scaling $\tau_d \sim N^{(1+2\nu_{2D})/(1+\nu_{2D})}$ obtained through the memory kernel approach violates the lower bound $\tau_d \sim N^{2\nu_{2D}}$, and therefore the former cannot be the correct scaling for τ_d . Indeed a short reflection makes the issue clear. The memory kernels we derived in Sec. 3 are actually “static memory kernels”: the individual monomer velocities involved, for determining the static memory kernels (i.e., for the equilibration process of the polymer when p extra monomers are injected at the pore, with $p \ll N$), are small, and as a result, the energy loss due to viscosity of the surrounding medium is negligible. For field-driven translocation in two-dimensions, since the lower bound for τ_d set by the viscous energy loss overrides the expression of τ_d obtained from the static memory kernel, it is very well possible that there exists a corresponding “dynamic memory kernel” that describes the relations between $\phi(t)$ and $v(t)$ for a translocating polymer.

We have not found a way to probe this dynamic memory kernel. We can nevertheless view its consequences by plotting the distance unthreaded $[s(t) - s(0)]$ as a function of t . We chose $h = 3$ for a variety of lengths of polymers (corresponding to strong confinement, i.e., equivalent to translocation in two dimensions driven by a strong field)

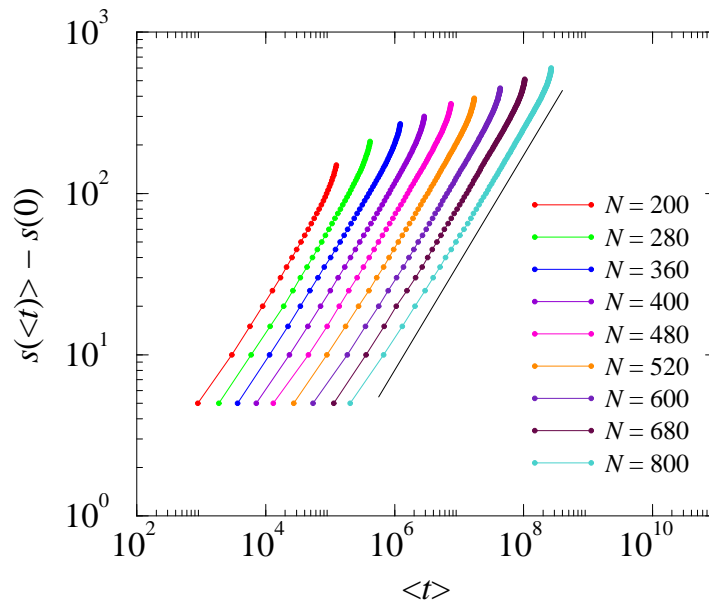


Figure 8. The mean time $\langle t \rangle$ required to unthread a distance $[s - s(0)]$ for $h = 3$, $h_1 = \infty$, $s(0) = 3N/4$ and $[s - s(0)] = 5, 10, \dots, N$. The $\langle t \rangle$ values are obtained as average over 2,048 realisations for each N . The N -values used are (from left to right): 200, 280, 360, 400, 480, 520, 600, 680, 800. The $\langle t \rangle$ -values for $N = 200$ is the actual value of time, for the others, $\langle t \rangle$ -values for each N are separated by a factor 2 along the x -axis. The solid line represents a power law with exponent $1/(2\nu_{2D})$, corresponding to $\tau_d \sim N^{2\nu_{2D}}$.

for this purpose. For a polymer of length N we hold $3N/4$ monomers between the plates $z = 0$ and $z = -h$, with the other $N/4$ monomers protruding out through the pore in the space $z > 0$, i.e., $s(0) = 3N/4$ [35]. We equilibrate both segments, and at $t = 0$ we let translocation begin. The mean time $\langle t \rangle$ required to unthread a distance $[s - s(0)]$ and the scaling of τ_d are presented in Fig. 8 and Table 5 respectively. We note that although $N^{2\nu_{2D}}$ provides only the lower bound for τ_d , our simulation data, along with those of Refs. [16, 23] suggests that $N^{2\nu_{2D}}$ is indeed the correct scaling for the τ_d in two dimensions.

6. Discussion

Polymer translocation out of confined spaces plays an important role for polymers in various biological processes. Planar confinements, however, are mostly a theoretical construct. In this paper, we have studied polymer translocation in three dimensions out of planar confinements, and demonstrated that polymer translocation in these (theoretically motivated) geometries is a very interesting testcase of fundamental physics of translocation dynamics.

The geometry we have considered is as follows. We have divided the three-dimensional space into two parts: $z > 0$ and $z < 0$ by a membrane placed at $z = 0$. This membrane is impenetrable to the polymer except for a narrow pore. We have then placed

N	τ_d	$\tau_u/N^{2\nu_{2D}}$
200	117934	41.6960
280	198497	42.3659
360	294199	43.0712
400	358865	44.8581
480	454131	43.1836
520	519663	43.8245
600	653885	44.4912
680	779484	43.9586
800	1026083	45.3469

Table 5. Median values of τ_d for $h = 3$, demonstrating $\tau_d \sim N^{2\nu_{2D}}$. The values are based on 2,048 translocation realisations for each N .

two more parallel membranes at $z = -h$ and $z = h_1$ that are completely impenetrable to the polymer. The polymer is initially sandwiched between the membranes placed at $z = -h$ and $z = 0$. We have considered strong confinement for the polymer, i.e., $h \ll R_g^{(3D)}$ where $R_g^{(3D)}$ is its radius of gyration in the bulk scaling as $\sim N^{\nu_{3D}}$. Here, N is the polymer length and $\nu_{3D} \simeq 0.588$ is the Flory exponent in three dimensions. Under these conditions the confined segment of the polymer essentially behaves as a polymer in two dimensions. If $h_1 > h$, the initial state of the polymer is entropically unfavourable, and the polymer escapes to the space between the membranes placed at $z = 0$ and $z = h_1$ through the pore in the membrane placed at $z = 0$: this is essentially the field-driven translocation process in two dimensions. We have studied two separate cases: (i) $h_1 = h$, and (ii) $h_1 = \infty$. For (i) the entropic drive is absent; the translocation dynamics reduces to that of an unbiased translocation for a two-dimensional polymer. Based on theoretical analysis and high-precision simulation data, we have shown that the dwell time τ_d , the time the pore remains occupied during translocation, scales as $N^{2+\nu_{2D}}$, in perfect agreement with our previous results. We have also shown that the probability distribution of the dwell time, $P(\tau_d)$ for $h_1 = h$ has a scaling form $P(\tau_d) \sim \mathcal{P}(\tau_d/N^{2+\nu_{2D}})/N^{2+\nu_{2D}}$. For (ii) we have shown that $\tau_d \sim N^{2\nu_{2D}}$, in agreement with several existing numerical results in the literature. Here $\nu_{2D} = 0.75$ is the Flory exponent in two dimensions. The result $\tau_d \sim N^{2\nu_{2D}}$ for case (ii) violates the earlier reported lower bound $1 + N^\nu$ for τ_d for field-driven translocation. We have argued, based on conservation of energy, that the actual lower bound for τ_d is $N^{2\nu}$ and not $1 + N^\nu$.

Acknowledgements

We gratefully acknowledge ample CPU time at the Dutch national supercomputer cluster SARA.

- [1] B. Dreiseikelmann, *Microbiol. Rev.* **58**, 293 (1994).
- [2] J. P. Henry *et al.*, *J. Membr. Biol.* **112**, 139 (1989).
- [3] J. Akimaru *et al.*, *PNAS USA* **88**, 6545 (1991).
- [4] D. Goerlich and T. A. Rappaport, *Cell* **75**, 615 (1993).
- [5] G. Schatz and B. Dobberstein, *Science* **271**, 1519 (1996).
- [6] I. Szabò *et al.* *J. Biol. Chem.* **272**, 25275 (1997).
- [7] B. Hanss *et al.*, *PNAS USA* **95**, 1921 (1998).
- [8] Yun-Long Tseng *et al.*, *Molecular Pharm.* **62**, 864 (2002).
- [9] J. Kasianowicz *et al.*, *PNAS USA* **93**, 13770 (1996).
- [10] J. J. Nakane, M. Akeson, A. Marziali, *J. Phys.: Cond. Mat.* **15**, R1365 (2003).
- [11] J. Buchner, *FASEB J.* **10**, 10 (1996); M. Magzoub, A. Pramanik and A. Gräslund, *Biochemistry* **44**, 14890 (2005); W. T. Wickner and H. F. Lodisch, *Science* **230**, 400 (1995); S. M. Simon and G. Blobel, *Cell* **65**, 1 (1991); D. Goerlich and I. W. Mattaj, *Science* **271**, 1513 (1996); K. Verner and G. Schatz, *Science* **241**, 1307 (1988); G. J. L. Wuite *et al.*, *Nature* **404**, 103 (2000).
- [12] B. H. Leighton *et al.*, *J. Biol. Chem.* **281**, 29788 (2006).
- [13] Y. Kafri, D. K. Lubensky, D. R. Nelson, *Biophys. J.* **86**, 3373 (2004).
- [14] W. Sung and P. J. Park, *Phys. Rev. Lett.* **77**, 783 (1996); S. K. Lee and W. Sung, *Phys. Rev. E* **63**, 012115 (2001); K. Lee and W. Sung, *Phys. Rev. E* **64**, 041801 (2001); M. Muthukumar, *J. Chem. Phys.* **111**, (1999); M. Muthukumar, *J. Chem. Phys.* **118**, 5174 (2003); M. Muthukumar, *Phys. Rev. Lett.* **86**, 3188 (2001); M. Muthukumar, *Electrophoresis* **23**, 2697 (2002); E. A. DiMarzio and J. J. Kasianowicz, *J. Chem. Phys.* **119**, 6378 (2003); E. Slonkina and A. B. Kolomeisky, *J. Chem. Phys.* **118**, 7112 (2003).
- [15] J. Chuang *et al.*, *Phys. Rev. E* **65**, 011802 (2001).
- [16] Y. Kantor and M. Kardar, *Phys. Rev. E* **69**, 021806 (2004).
- [17] K. Luo *et al.*, *J. Chem. Phys.* **124**, 034714 (2006).
- [18] D. Wei *et al.*, *J. Chem. Phys.* **126**, 204901 (2006).
- [19] J. Klein Wolterink, G. T. Barkema and D. Panja, *Phys. Rev. Lett.* **96**, 208301 (2006).
- [20] A. Milchev, K. Binder, and A. Bhattacharya, *J. Chem. Phys.* **121**, 6042 (2004).
- [21] J. L. A. Dubbeldam *et al.*, *Phys. Rev. E* **76**, 010801(R) (2007).
- [22] K. Luo *et al.*, *J. Chem. Phys.* **124**, 114704 (2006); I. Huopaniemi *et al.*, *J. Chem. Phys.* **125** 124901 (2006); K. Luo *et al.*, e-print arxiv 0708.1147.
- [23] A. Cacciuto and E. Luijten, *Phys. Rev. Lett.* **96**, 238104 (2006).
- [24] J. L. A. Dubbeldam *et al.*, *Europhys. Lett.* **79**, 18002 (2007).
- [25] R. Metzler and J. Klafter, *Biophys. J.* **85** 2776 (2003).
- [26] D. Panja, G. T. Barkema and R. C. Ball, e-print arXiv: cond-mat/0703404; to appear in *J. Phys.: Cond. Mat.* (2007).
- [27] D. Panja, G. T. Barkema and R. C. Ball, e-print arXiv: cond-mat/0610671 (version 2).
- [28] D. Panja and G. T. Barkema, e-print arXiv: 0706.3969; to appear in *Biophys. J.* (2007).
- [29] E. F. Casassa, *J. Polym. Sci., Part B: Polym. Lett.* **5**, 773 (1967); S. F. Edwards and K. F. Freed, *J. Phys. A* **2**, 145 (1969).
- [30] P.-G. de Gennes, *Scaling concepts in polymer physics* (Cornell University Press, New York, 1979).
- [31] P.-G. de Gennes, *Proc. Natl. Acad. Sci. USA* **96**, 7262 (1999); D. E. Smith. *et al.*, *Nature* **413**, 748 (2001); J. Arsuaga *et al.*, *Proc. Natl. Acad. Sci. USA* **102**, 9165 (2005).
- [32] A. van Heukelum and G. T. Barkema, *J. Chem. Phys.* **119**, 8197 (2003); A. van Heukelum *et al.*, *Macromol.* **36**, 6662 (2003); J. Klein Wolterink *et al.*, *Macromol.* **38**, 2009 (2005); J. Klein Wolterink and G. T. Barkema, *Mol. Phys.* **103**, 3083 (2005).
- [33] For unbiased translocation, EN in this argument is to be replaced by the difference in free energy (or entropy) of a threaded polymer, corresponding to $s = N/2$, and the translocated polymer, corresponding to $s = N$. This leads to the inequality $\tau_d \geq \eta N^{1+2\nu}$.
- [34] We have checked, for $h = 3$, using the proxy variable $Z^{(4)}$ for Φ as in Fig. 3(a) of Ref. [28], that $[\phi(0) - \phi(t)]$ indeed remains a constant throughout translocation, aside from some small values

of t .

[35] We have checked that the scaling results are not influenced by whether $s(0) = N/4$ or $N/2$.